Electronic Supplementary Material (ESI) for Chemical Communications.

Supporting Information

Strategic design of an NIR probe for viscosity imaging in inflammatory and non-alcoholic steatohepatitis mice

Yaogeng Ma,[a] Min Li,[a] Huilin Sun,[b] Jing-Yuan Ge,*[a] Yang Bai,*[b] Lin Qiu,[b] Xuan Wu,*[c] Jiuxi Chen[a] and Zhongyan Chen*[a]

[a] College of Chemistry and Materials Engineering, Wenzhou University, Wenzhou 325035, P. R. China. Email: gejingyuan90@126.com; chenzhongyan@wzu.edu.cn

[b] School of Pharmacy, Changzhou University, Changzhou 213164, P. R. China. Email: baiy@cczu.edu.cn.

[c] School of Chemistry & Chemical Engineering, Yangzhou University, Yangzhou 225002, P. R. China. Email: wuxuan1119@yzu.edu.cn.

1. Materials and instruments

Unless otherwise stated, all reagents were purchased from commercial suppliers (Aladdin, Sigma-Aldrich, and TCI) and used without further purification. The silica gels (100-200 and 300-400 mesh) and neutral aluminum oxide (200–300 mesh) were purchased from Qingdao Ocean Chemical Co. Ltd. High fat food (methionine-choline deficient diet) comes from Jiangsu Xietong pharmaceutical bio-engineering Co., Ltd. Fluorescence spectrum were recorded using a Hitachi F-4700 FL spectrophotometer. Absorption spectra were recorded using a Shimadzu UV-2600 spectrophotometer. ^{1}H NMR and ^{13}C NMR spectra were measured on 400, 500 or 600 MHz Bruker spectrometer. Mass spectrometric data were acquired on a microTOF-QII HRMS/MS instrument (BRUKER). Viscosity values of methanol-glycerol systems in different proportions were measured with a NDJ-8S rotational viscometer. All media pH measurements were determined by a Model PHS-3E meter. The fluorescence images of cells were determined using a Nikon Ti2 confocal fluorescence microscope (Japan) with 60× oil immersion objective. The fluorescence images of mice were collected on a Perkin Elmer IVIS Lumina XRMS Series III (U.S.)

2. Synthesis and characterization of probes

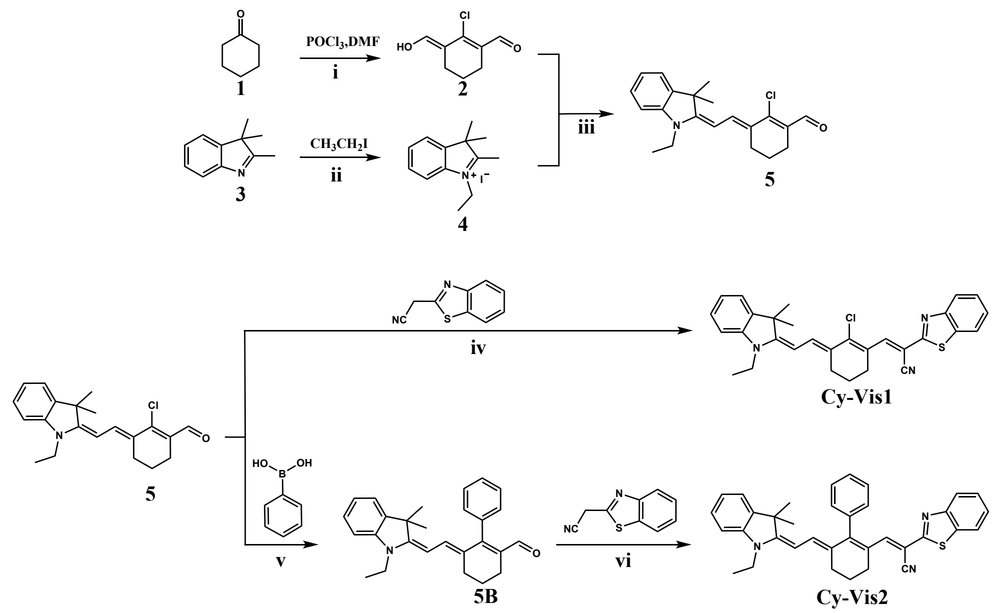

Scheme S1. Synthesis of **Cy-Vis1** and **Cy-Vis2**. Reagents and conditions:(i) $POCl_3$, DCM:DMF = 1:1(v/v), 80 ^oC, reflux, 24 hours; (ii) Toluene, reflux, 24 hours; (iii) Toluene/acetic acid = 3:1 (v/v), 110 ^oC, 2 hours. (iv) Piperidine, EtOH, reflux. (v) K_3PO_4, $Pd(PPh_3)_4$, DMF: H_2O = 5:1(v/v), 120 °C, 24 hours. (vi) Piperidine, EtOH, reflux.

Synthesis of Compound 2. To a solution of DMF (18 mL) in DCM (18 mL), $POCl_3$ (15 mL, 161 mmol) was added dropwise at -10 ^oC. After 1 hour, cyclohexanone (4.5 mL, 43 mmol) was added, and the mixture was heated to 80 ^oC for 12 hours. The mixture solution was poured into ice water, and kept it overnight. The precipitate was filtered to obtain **2** as a yellow solid (4.9 g, 66.1%).

Synthesis of Compound 4. 2, 3, 3-trimethyl-indolenine (7.2 mL, 45 mmol) and iodoethane (6 mL, 75 mmol) were dissolved in toluene (60 mL). The mixture solution was refluxed for 24 hours. After being cooled to room temperature, the solid was filtered and washed with ethyl acetate to obtain **4** as a red solid (8.7 g, 61.5%).

Synthesis of Compound 5. Compounds **2** (344 mg, 2 mmol) and **4** (630 mg, 2 mmol) were dissolved in a mixture of toluene and acetic acid (20 mL, v/v = 3:1). The mixture solution was stirred at 110 °C for 2 hours. After cooling to room temperature, the mixture was poured into water and extracted with ethyl acetate (50 mL× 3). The organic layer was dried over anhydrous Na_2SO_4. Aluminum oxide column purification was performed by using PE/EA = 20:1 to obtain compound **5** as a red solid (282.5 mg, 41.3%).**^{1}H NMR** (400 MHz, $CDCl_3$, δ): 10.25 (s, 1H), 7.84 (d, J = 12.0 Hz, 1H), 7.21 (d, J = 4.0 Hz, 2H), 6.95 (t, J = 8.0 Hz, 1H), 6.72 (d, J = 4.0 Hz, 1H), 5.52 (d, J = 12.0 Hz, 1H), 3.75 (d, J = 8.0 Hz, 2H), 2.60 (t, J = 4.0 Hz, 2H), 2.49 (t, J = 4.0 Hz, 2H), 1.74-1.81 (m, 2H) , 1.66 (s, 6H), 1.28 (t, J = 8.0 Hz, 3H). **^{13}C NMR** (100 MHz, $CDCl_3$, δ): 190.8, 161.6, 148.7, 143.5, 139.4, 131.4, 128.4, 127.9, 122.9, 121.8, 120.8, 106.7, 92.4, 46.5, 37.1, 28.3, 26.7, 24.5, 20.9, 11.1. **HRMS** (ESI, m/z) calcd. 342.1619, found 342.1629 for $[M+H]^+$.

Synthesis of Compound 5B. Compound **5** (136.7 mg, 0.4 mmol), Phenylboronic acid (195.1 mg, 1.6 mmol), and K_3PO_4 (987.2 mg, 4.7 mmol) $Pd(PPh_3)_4$ (190 mg, 0.16 mmol) DMF and H_2O (25 mL, v/v = 5:1). The mixture solution was stirred at 120 °C for 24 hours. After cooling to room temperature, the mixture was dissolved in ethyl acetate (50 mL) and washed with brine (3×100 mL). The organic layer was dried over Na_2SO_4, and concentrated under reduced pressure. Aluminum oxide column purification was performed by using PE/EA = 20:1 to obtain compound **5B** as a orange solid (121.5 mg, 79.2%).**^{1}H NMR** (400 MHz, $CDCl_3$, δ): 9.26 (s, 1H), 7.41 (t, J = 8.0 Hz, 3H,), 7.22 (d, J = 4.0 Hz, 2H), 7.15 (t, J = 8.0 Hz, 1H), 7.03 (d, J = 8.0 Hz, 1H), 6.85 (t, J = 8.0 Hz, 1H), 6.63 (d, J = 8.0 Hz, 1H), 6.46 (d, J = 12.0 Hz, 1H), 5.50 (d, J = 12.0 Hz, 1H), 3.68 (q, J = 8.0 Hz, 2H), 2.61 (t, J = 8.0 Hz, 2H), 2.57 (t, J = 4.0 Hz, 2H), 1.90-1.84 (m, 2H), 1.24 (t, J = 4.0 Hz, 3H), 1.10 (s, 6H). **^{13}C NMR** (100 MHz, $CDCl_3$, δ) 193.0, 160.1, 158.4, 143.6, 139.3, 137.5, 133.8, 131.5, 130.2, 128.8, 127.8, 127.7, 127.4, 121.6, 120.3, 106.4, 92.4, 45.8, 37.0, 27.8, 25.4, 22.4, 21.4, 11.1. **HRMS** (ESI, m/z) calcd. 384.2322, found 384.2358 for $[M+H]^+$.

Synthesis and characterization of Cy-Vis1. Compound **5** (341.8 mg, 1 mmol), Benzothiazole-2-acetonitrile (261.4 mg, 1.5 mmol), and piperidine (0.1 mL) were dissolved in EtOH (10 mL). the mixture solution was heated at reflux for 12 hours. After cooling to room temperature, the solution was concentrated under reduced pressure. The mixture was dissolved in CH_2Cl_2 (50 mL) and washed with brine (3×50 mL). The organic layer was dried over Na_2SO_4, and concentrated under reduced pressure. Silica gel column purification was performed by using PE/DCM = 1:3 as the eluent to obtain compound **Cy-Vis1** as a green solid (368.0 mg, 73.9%). ^{1}H NMR (400 MHz, $CDCl_3$, δ): 8.62 (s, 1H), 8.04 (d, *J* = 8.0 Hz, 1H), 7.83 (t, *J* = 8.0 Hz, 2H), 7.47 (t, *J* = 8.0 Hz, 1H), 7.36 (t, *J* = 8.0 Hz, 1H), 7.22 (d, *J* = 8.0 Hz, 2H), 6.97 (t, *J* = 8.0 Hz 1H), 6.74 (d, *J* = 8.0 Hz, 1H), 5.58 (d, *J* = 12.0 Hz 1H), 3.78 (d, *J* = 8.0 Hz 2H), 3.09 (t, *J* = 8.0 Hz 2H), 2.60 (t, *J* = 8.0 Hz 2H), 1.92 (t, *J* = 8.0 Hz, 2H), 1.67 (s, 6H), 1.30 (t, *J* = 4.0 Hz, 3H). ^{13}C NMR (150 MHz, $CDCl_3$, δ) 165.5, 162.1, 154.0, 144.9, 144.2, 143.2, 139.5, 134.7, 133.2, 127.9, 126.4, 125.8, 125.1, 124.2, 123.1, 121.8, 121.3, 121.2, 118.2, 107.0, 99.9, 93.7, 46.7, 37.2, 28.4, 28.2, 26.0, 21.3, 11.2. HRMS (ESI, m/z) calcd. 498.1765, found 498.1764 for $[M+H]^+$.

Synthesis and characterization of Cy-Vis2. Compound **5B** (95.9 mg, 0.25 mmol), Benzothiazole-2-acetonitrile (65.4 mg, 0.375 mmol), and piperidine (25 μL) were dissolved in EtOH (2.5 mL) the mixture solution was heated at reflux for 12 hours. After cooling to room temperature, the solution was concentrated under reduced pressure. The mixture was dissolved in CH_2Cl_2 (30 mL) and washed with brine (3×30 mL). The organic layer was dried over Na_2SO_4, and concentrated under reduced pressure. Silica gel column purification was performed by using PE/EA = 20:1 as the eluent to obtain compound **Cy-Vis2** as a blue solid (79.8 mg, 59.1%). ^{1}H NMR (400 MHz, $CDCl_3$, δ): 7.90 (d, *J* = 8.0 Hz, 1H), 7.69 (d, *J* = 8.0 Hz, 1H), 7.51-7.46 (m, 4H), 7.38 (t, *J* = 8.0 Hz, 1H), 7.28-7.24 (m, 1H), 7.20 (d, *J* = 8.0 Hz, 2H), 7.16 (d, *J* = 8.0 Hz, 1H), 7.04 (d, *J* = 8.0 Hz, 1H), 6.88 (t, *J* = 8.0 Hz, 1H), 6.66 (d, *J* = 8.0 Hz, 1H), 6.45 (d, *J* = 12.0 Hz, 1H), 5.55 (d, *J* = 12.0 Hz, 1H), 3.71 (q, *J* = 8.0 Hz, 2H), 3.10 (t, *J* = 8.0 Hz, 2H), 2.60 (t, *J* = 8.0 Hz, 2H), 2.00 (t, *J* = 8.0 Hz, 2H), 1.25 (t, *J* = 8.0 Hz, 3H), 1.10 (s, 6H). ^{13}C NMR (125 MHz, $CDCl_3$, δ) 166.1, 160.7, 155.9, 153.9, 147.9, 143.3, 139.3, 138.9, 135.9, 134.1, 130.1, 129.6, 128.5, 128.0, 127.7, 127.6, 126.0, 124.7, 122.8, 121.5, 120.9, 120.7, 118.2, 106.6, 97.5, 93.4, 46.0, 37.0, 27.7, 26.8, 24.6, 21.7, 11.1. HRMS (ESI, m/z) calcd. 540.2468, found 540.2488 for $[M+H]^+$.

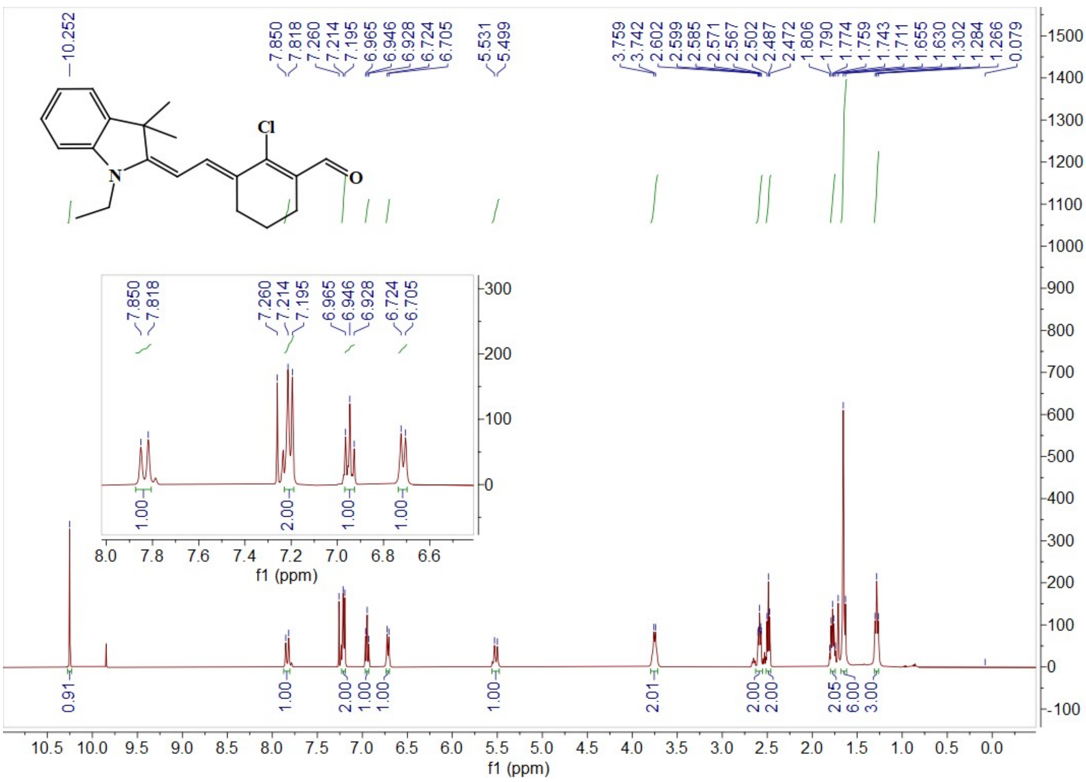

Fig. S1. ^{1}H NMR spectrum of **5** in $CDCl_3$.

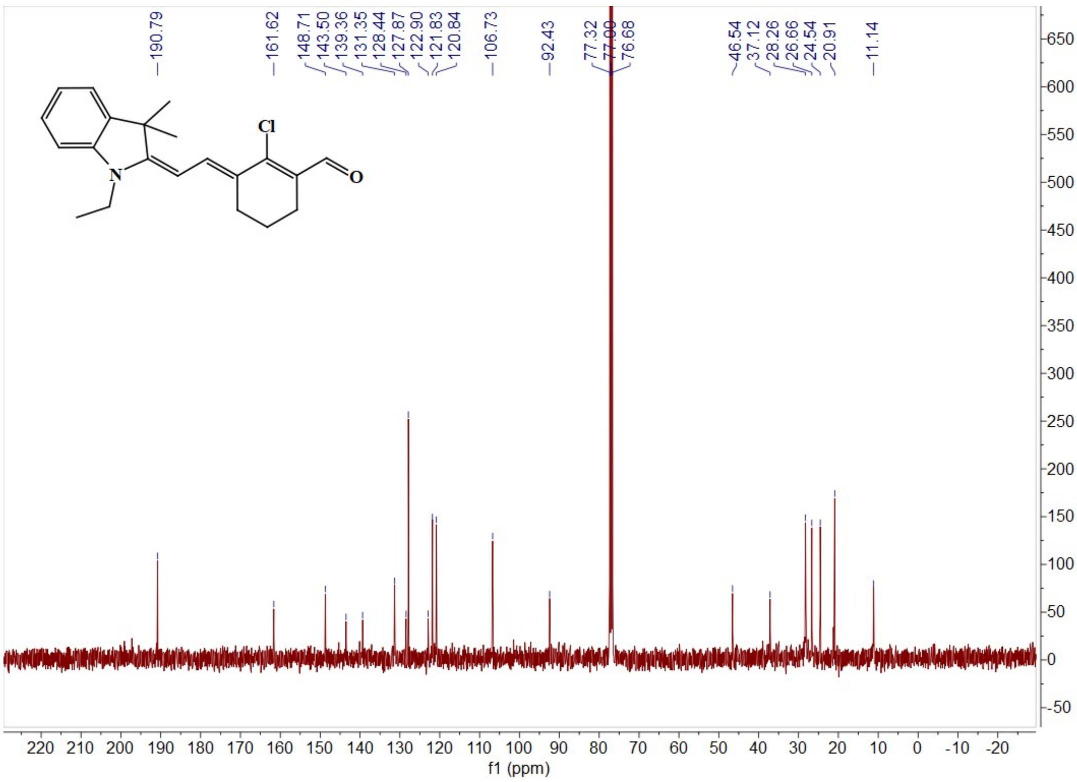

Fig. S2. ^{13}C NMR spectrum of **5** in $CDCl_3$.

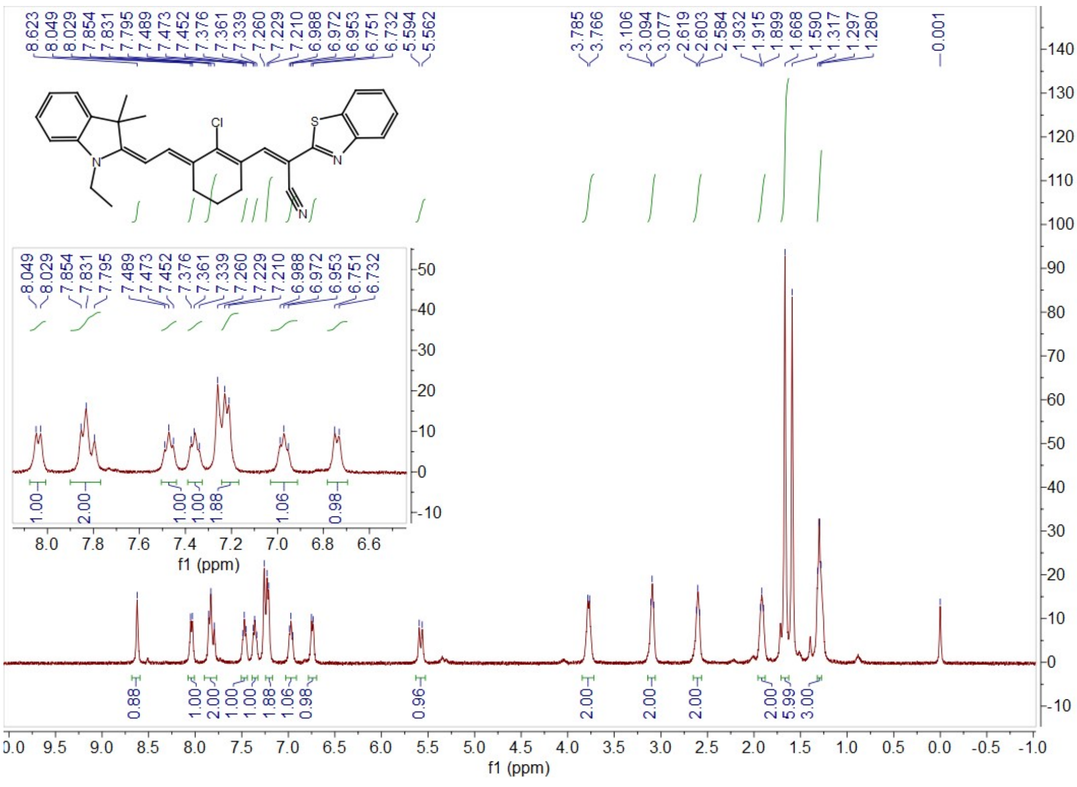

Fig. S3. ^{1}H NMR spectrum of **Cy-Vis1** in $CDCl_3$.

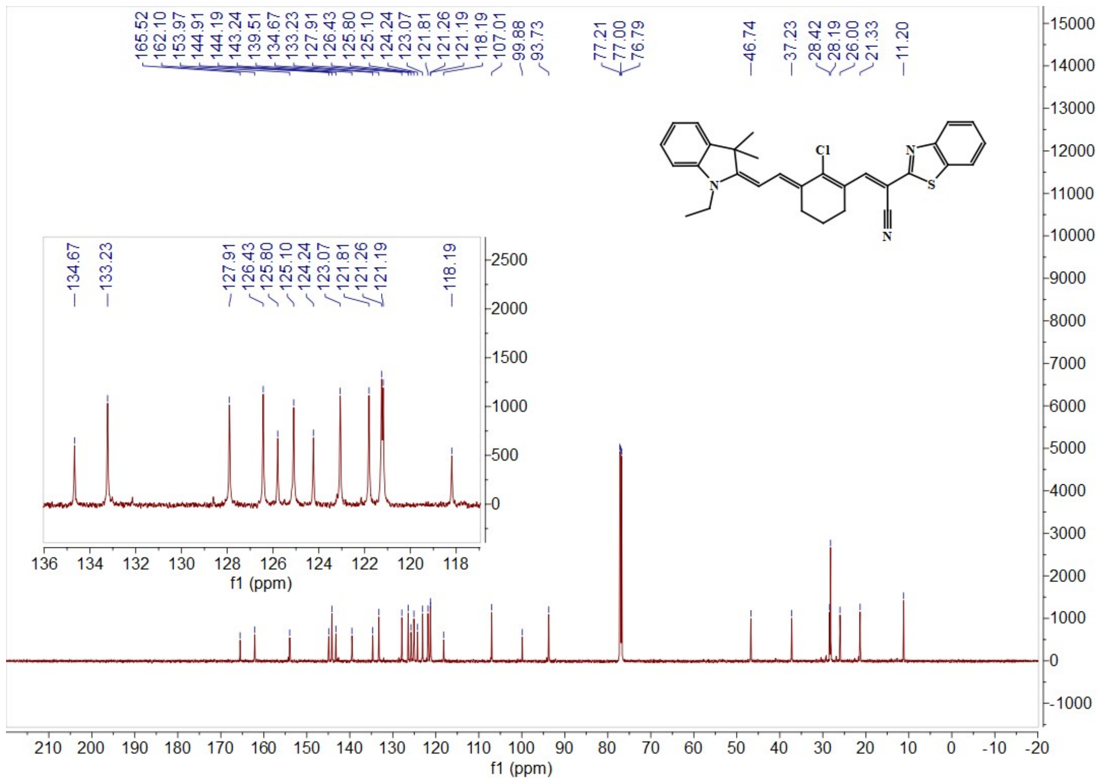

Fig. S4. ^{13}C NMR spectrum of **Cy-Vis1** in $CDCl_3$.

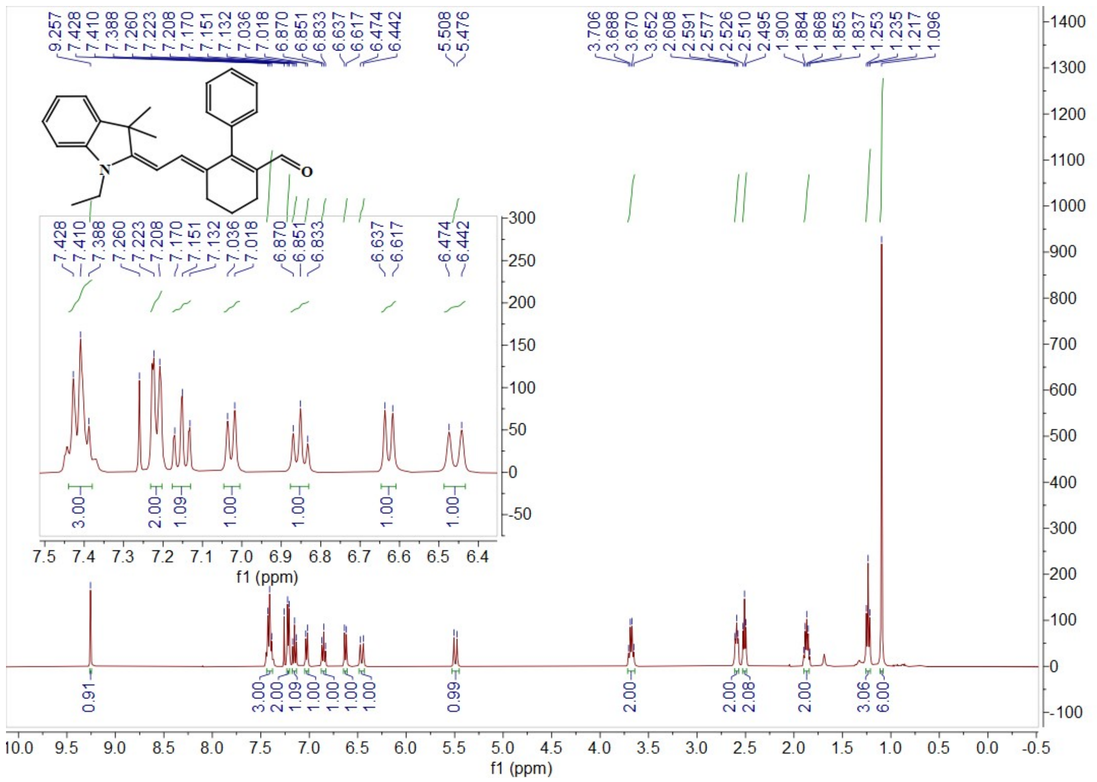

Fig. S5. ^{1}H NMR spectrum of **5B** in $CDCl_3$.

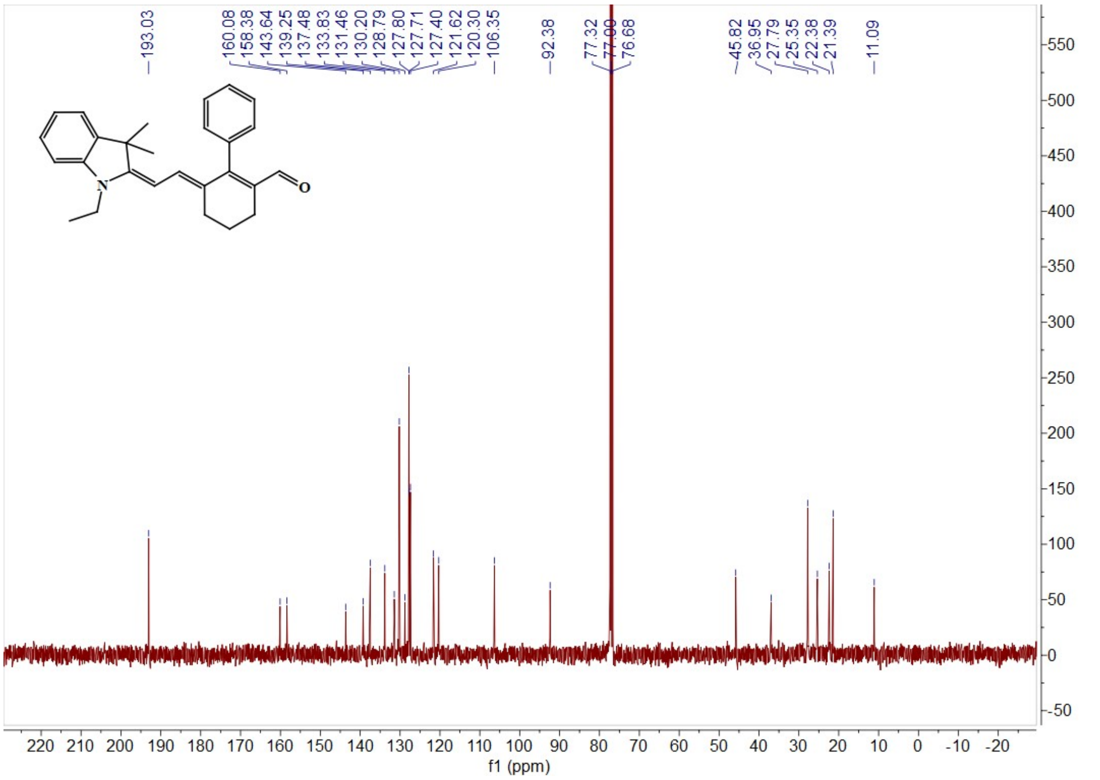

Fig. S6. ^{13}C NMR spectrum of **5B** in $CDCl_3$.

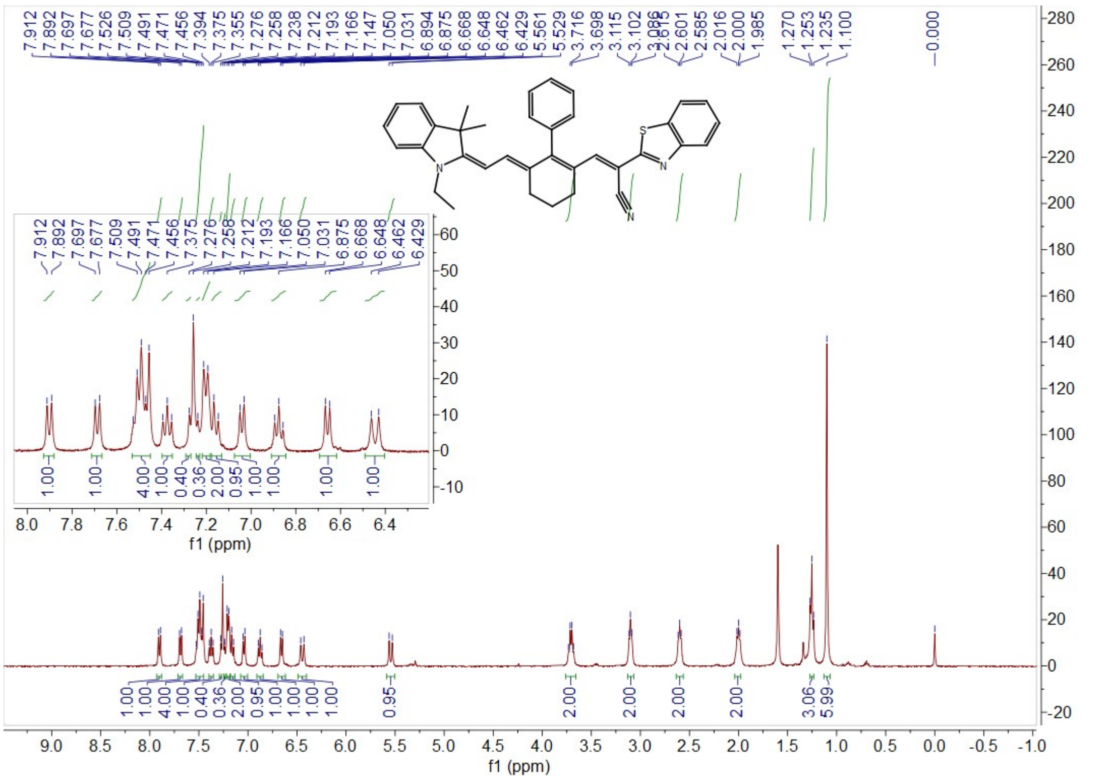

Fig. S7. ^{1}H NMR spectrum of **Cy-Vis2** in $CDCl_3$.

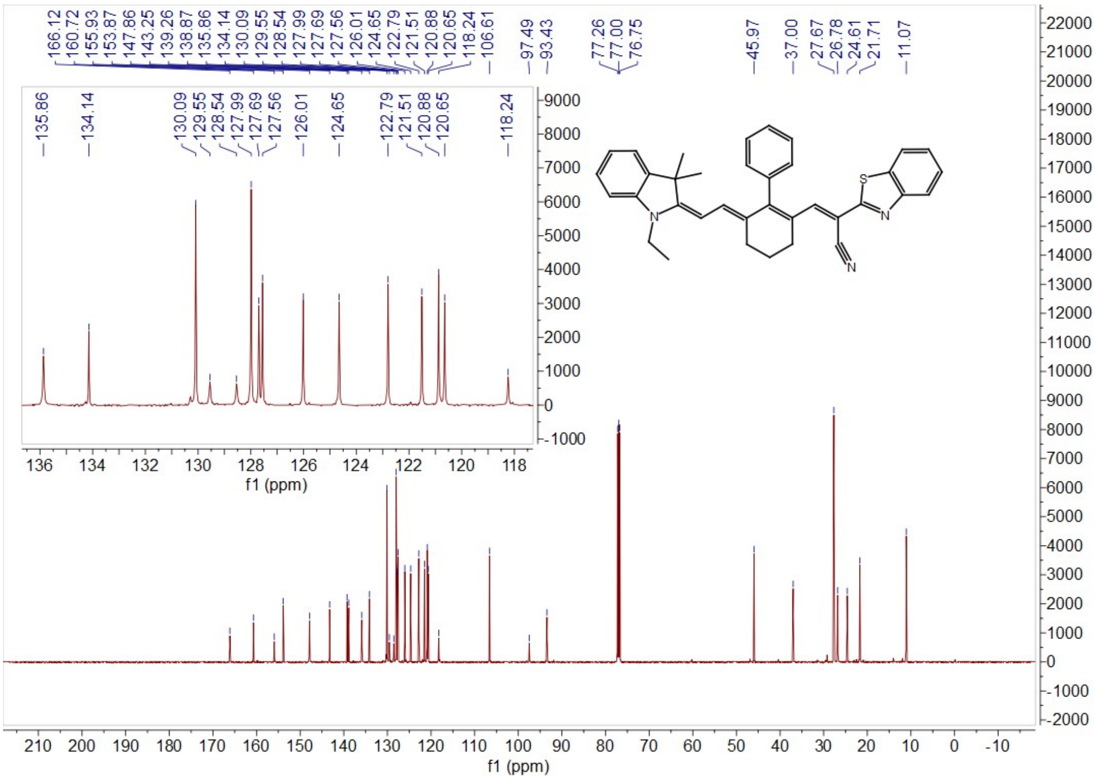

Fig. S8. ^{13}C NMR spectrum of **Cy-Vis2** in $CDCl_3$.

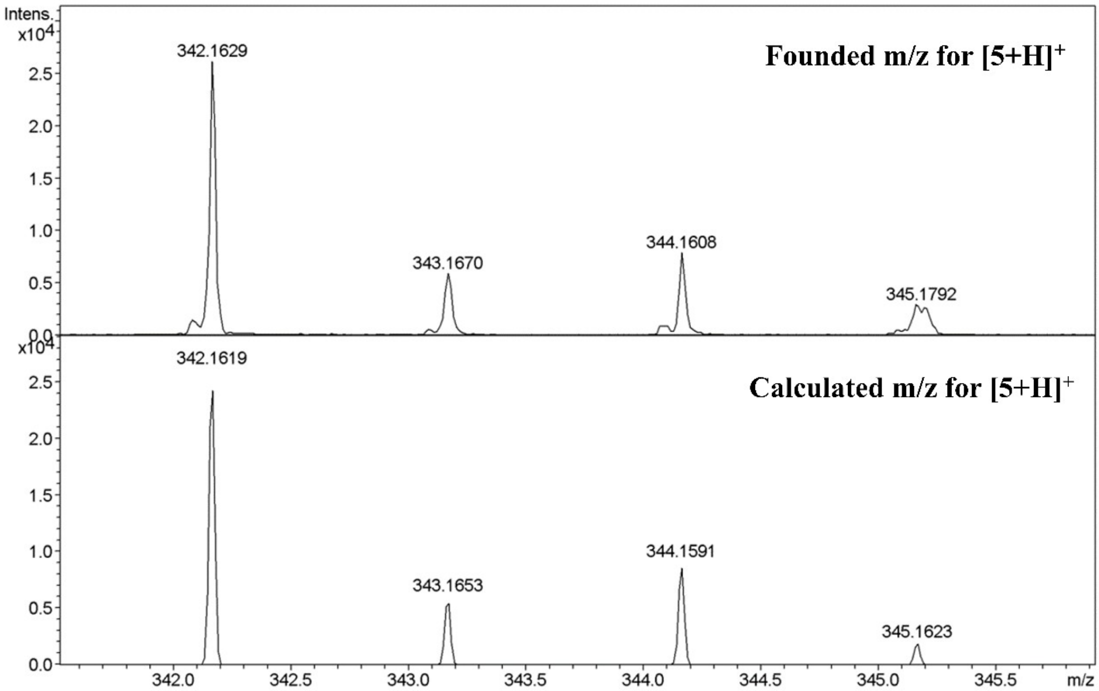

Fig. S9. Comparisons of observed m/z peaks with calculated m/z for [**5**+H]$^+$.

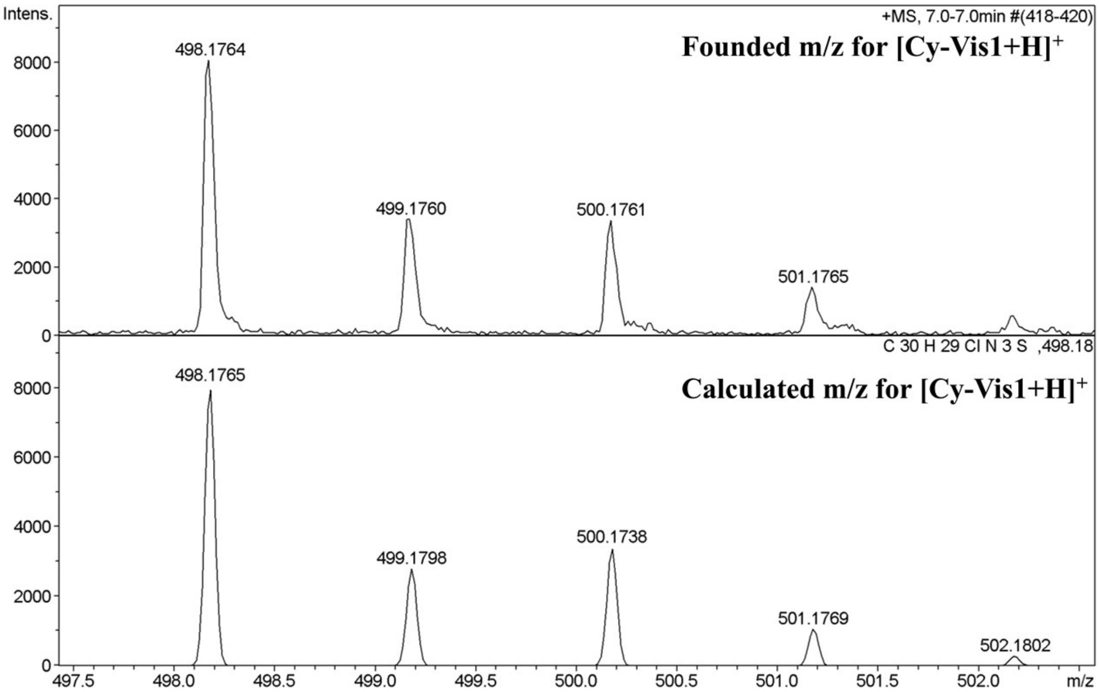

Fig. S10. Comparisons of observed m/z peaks with calculated m/z for [**Cy-Vis1**+H]$^+$.

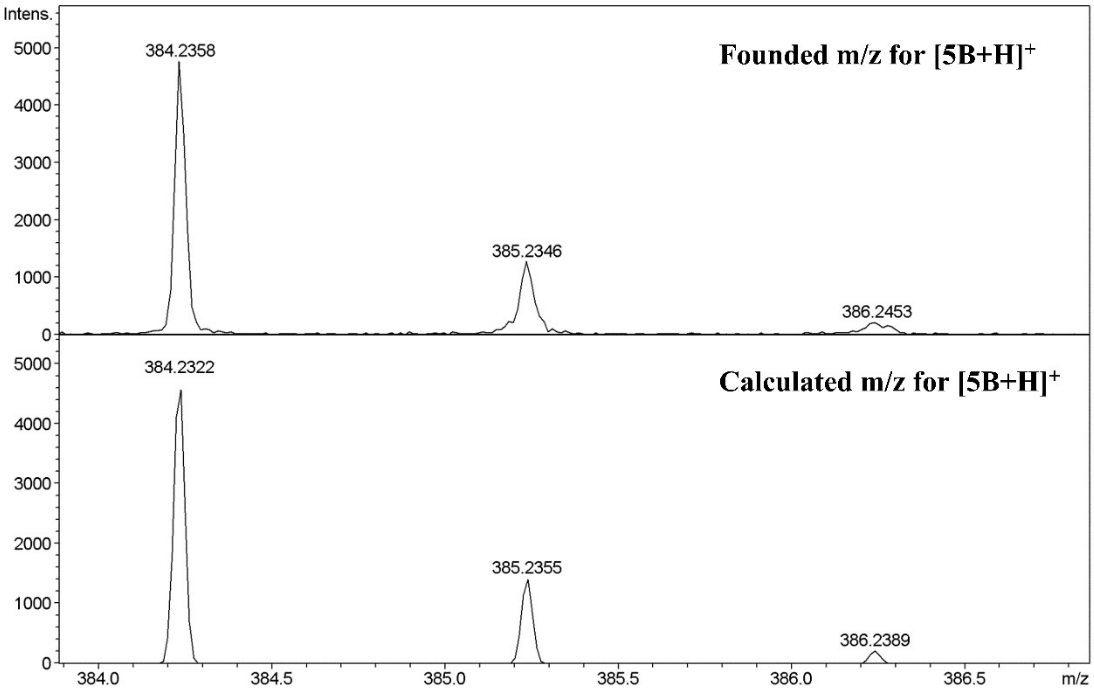

Fig. S11. Comparisons of observed m/z peaks with calculated m/z for [**5B**+H]$^+$.

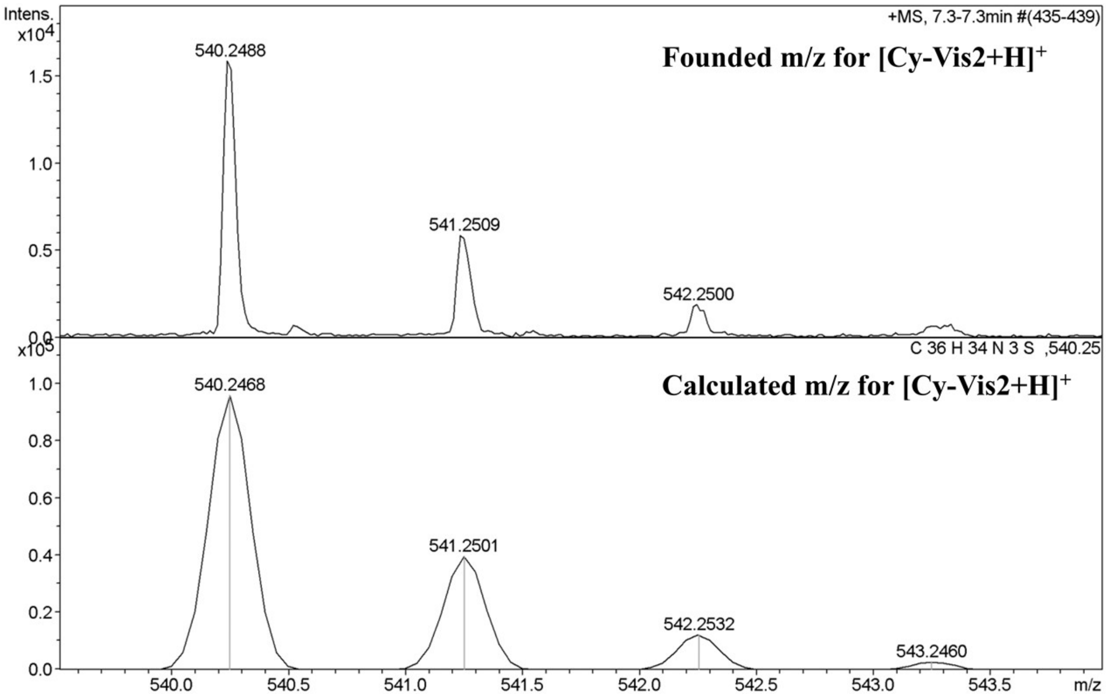

Fig. S12. Comparisons of observed m/z peaks with calculated m/z for [**Cy-Vis2**+H]$^+$.

3. Quantum chemical calculations

All calculations are performed using Gaussian16 package.[1] The ground-state geometries were fully optimized using the density functional theory (DFT) with B3LYP-D3(BJ) functional at the basis set level of 6-311G (d,p). To consider the solvent effect, methanol was used as the solvent. All calculations were based on the polarizable continuum model (PCM). Analyze wavefunction with Multiwfn and visualize it with VMD.[2]

4. Fluorescence quantum yield measurement

The fluorescence quantum yield (QY) was determined according to following equation[3]:

$$\Phi_x = \frac{n_x^2}{n_s^2} \cdot \frac{A_s \cdot F_x}{A_x \cdot F_s} \cdot \Phi_s$$

where Φ_s was the QY of reference, F was the Integrated area of emission spectrum, A was the absorbance at the excitation wavelength, and n was the refractive index of the used solvent. "x" and "s" stand for compounds and reference, respectively. The fluorescence quantum yield was determined by measuring emission spectrum with Sulforhodamine 101 in MeOH (Φ_s = 0.91) as a reference[4].

Table S1 Properties of representative NIR fluorescent probes for viscosity imaging

No	Structure and Ref	λex/λem	Stokes shifts	Response signal	Imaging scale	Disease model
This work	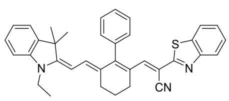 Cy-Vis2	611/737	126 nm	20-fold	Cell line Mice	Inflammatory; Non-alcoholic steatohepatitis
1	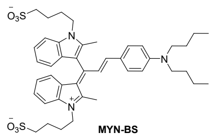 MYN-BS Chem. Commun., 2022, 58, 12815	670/710	40 nm	36-fold	Cell line	None
2	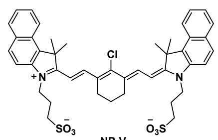 NP-V J. Am. Chem. Soc., 2022, 144, 13586	820/864	44 nm	13-fold	Cell line Mice	Hepatic ischemia−reperfusion injury
3	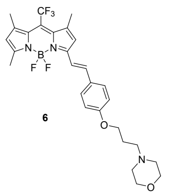 6 Sens. Actuators. B Chem., 2022, 359, 131594	610/657	47 nm	-	Cell line	None
4	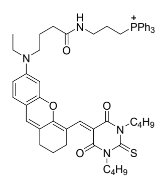 MC-TB-Mito Mater. Chem. Front., 2021, 5, 2459	640/700	60 nm	9-fold	Cell line	None

5	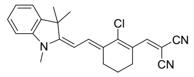 NLV-1 Sens. Actuators. B Chem., 2018, 271, 321	650/719	69	14-fold	Cell line Zebra fishes Mice	Inflammatory
6	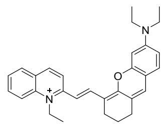 QX-V Anal. Chim. Acta, 2023, 1242, 340813	710/786	76 nm	43-fold	Cell line Mice	Tumor; Fatty-liver
7	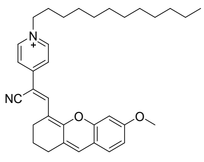 DHX-V-C_{12} Anal. Chem., 2023, 95, 7254	590/675	85 nm	449-fold	Cell line Mice tissue	Inflammatory
8	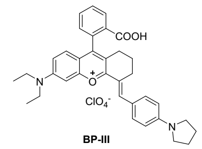 BP-III Chem. Eng. J., 2022, 445, 136448	649/740	91 nm	200-fold	Cell line Mice	Fatty-liver
9	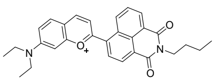 V-M1 Chem. Commun., 2020,56, 6684	505/650	145 nm	3-fold	Cell line Mice	Tumor
10	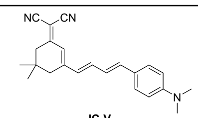 IC-V Chem. Commun., 2023, 59, 5607	530/700	170 nm	180-fold	Cell line Mice	Tumor

5. Photophysical properties of Cy-Vis1 and Cy-Vis2

The stock solution of **Cy-Vis1** and **Cy-Vis2** were prepared in DMSO (1 mM) and stored at 4 ^{o}C. The absorption and fluorescence spectra of 10 μM probes were performed in solvents with different polarities. For viscosity response experiments, the emission spectra were performed in different percentage of glycerin (Gly) and methanol solution (v/v). For selective response, the emission spectra were recorded in 20 mM HEPES buffer solution (10% DMSO, v/v, pH 7.4) and methanol/glycerol (1/1, v/v) upon addition of different analytes. For pH response experiments, the emission spectra were measured in HEPES buffer - glycerin mixture solution (1:1, v/v) at different pH value (pH 4.42 – 12.01). The solution pH was adjusted by 1 M NaOH or 1 M HNO_3. For the emission spectra measurements, the excitation wavelength was 600 nm, the excitation slit widths and emission slit widths were 5 nm.

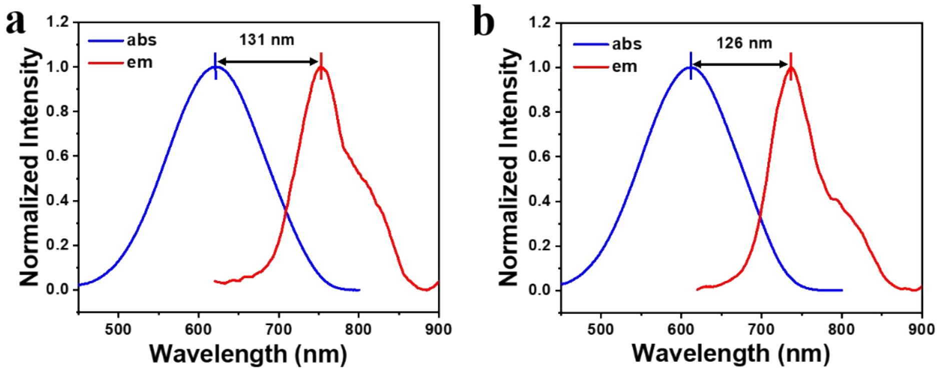

Fig. S13. Normalized absorption and emission spectra of **Cy-Vis1** (a) and **Cy-Vis2** (b) in methanol.

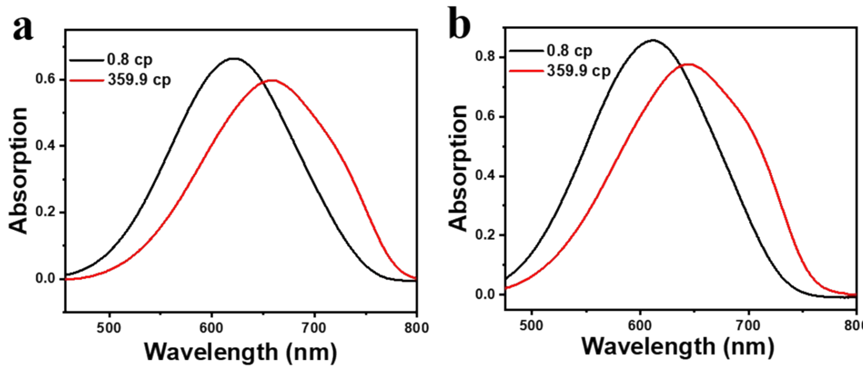

Fig. S14. UV–Vis absorption of **Cy-Vis1** (a) and **Cy-Vis2** (b) in methanol−glycerol systems with different viscosities.

Table S2 Spectroscopic and viscosity data

Probe	λ_{abs} (nm)[a]	λ_{em} (nm)[a]	Stokes shifts (nm)[a]	Φ_F (%)[a]	Φ_F (%)[b]	Fold[c]
Cy-Vis1	622	753	131	0.06	0.37	7.6
Cy-Vis2	611	737	126	0.11	1.28	19.9

[a] Spectroscopic data measured in methanol; [b] Spectroscopic data measured in 90% glycerol; [c] Fold increase in fluorescence intensity from 0.8 cp (methanol) to 359.9 cp (90% glycerol).

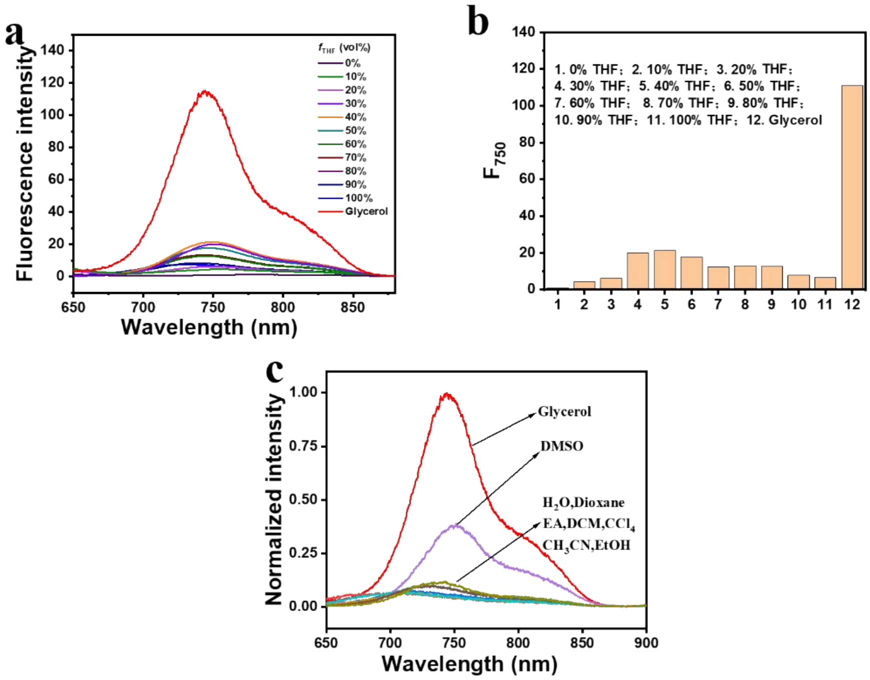

Fig. S15.(a) Fluorescence spectra of 10 μM **Cy-Vis2** in THF-H_2O systems. (b) Intensity of **Cy-Vis2** at 750 nm in THF-H_2O systems. (c) Fluorescence spectra of 10 μM **Cy-Vis2** in different solvents.

Table S3 Dielectric constants of binary mixed solvents and normalized fluorescence intensity

H_2O/THF (v/v)	Polarity (ε)	Normalized fluorescence intensity
10:0	78.4	0.045
9:1	71.3	0.212
8:2	64.2	0.292
7:3	57.1	0.936
6:4	50	1.000
5:5	42.9	0.831
4:6	35.8	0.588
3:7	28.7	0.616
2:8	21.6	0.591
1:9	14.5	0.373
0:10	7.4	0.314

Table S4 Dielectric constants and viscosity coefficients η of different solutions and normalized fluorescence intensity

Solution	Polarity (ε)	Viscosity (cp)	Normalized fluorescence intensity
Glycerol	42.5	923.9	1.000
DMSO	46.8	2.0	0.386
H_2O	78.4	0.9	0.053
Dioxane	2.2	1.1	0.046
EA	6.0	0.8	0.041
DCM	8.9	0.8	0.085
CCl_4	2.2	1.3	0.040
CH_3CN	35.7	0.6	0.103
EtOH	24.9	1.0	0.085
MeOH	32.6	0.8	0.102
THF	7.4	0.7	0.060

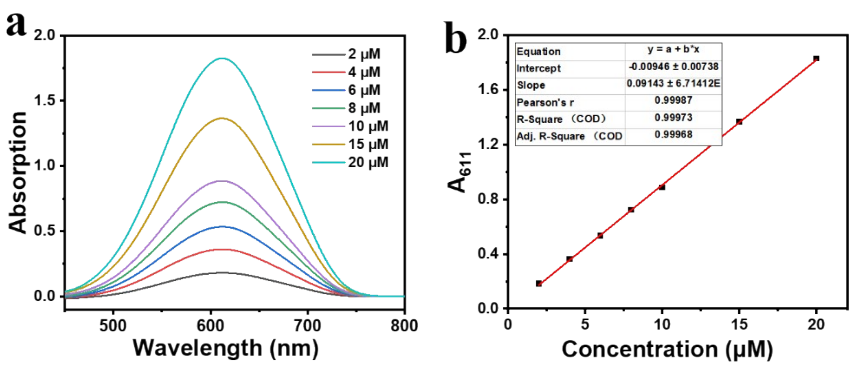

Fig. S16. (a) Absorption spectra of **Cy-Vis2** in MeOH with different concentrations. (b) Standard curve of absorbance at 611 nm with concentration.

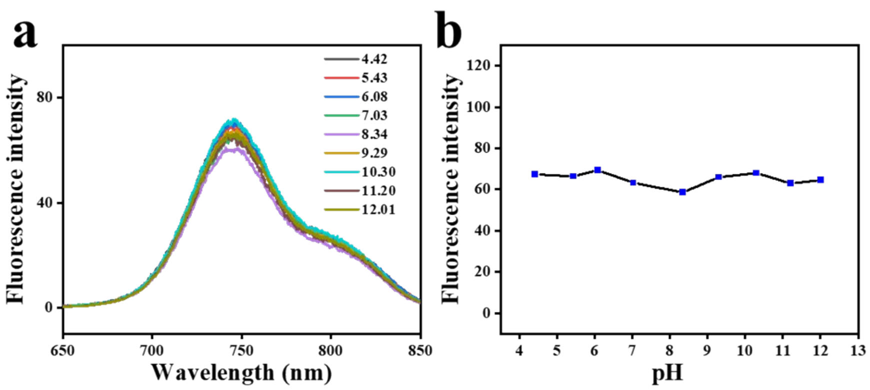

Fig. S17. (a) The emission spectra of **Cy-Vis2** (10 μM) in HEPES buffer-glycerin mixture solution (1:1, v/v) with different pH value. (b) Intensity of **Cy-Vis2** at 750 nm with different pH value.

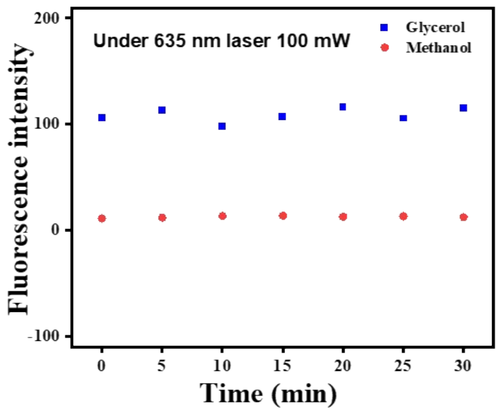

Fig. S18. Intensity of 10 μM **Cy-Vis2** at 750 nm upon illumination of 635 nm laser (100 mW/cm^2) in glycerol or methanol, respectively.

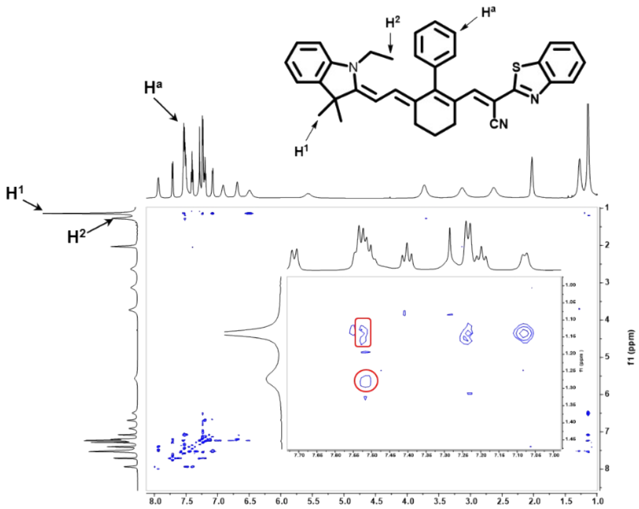

Fig. S19 Two-dimensional ^{1}H NOESY spectrum of **Cy-Vis2** in $CDCl_3$. Intramolecular correlation signals of H^a to H^1 and H^2 are circled in red.

6. Fluorescence microscopy of HepG2 cells

HepG2 cells were pretreated with 5 μM LPS or 150 μM oleic acid (OA) for 4 h at 37 °C and washed with PBS for 3 times. Then the cells were incubated with **Cy-Vis2** (5 μM in PBS containing 2% DMSO) for 1 h at 25 °C. Then the cells were washed with PBS for 3 times before imaging under confocal fluorescence microscope with 60× oil immersion objective. Fluorescent images were collected from 650 to 1000 nm with excitation wavelength at 560 nm.

7. In vivo imaging of mice

All animal experiments in vivo are performed in strict accordance with the ARRIVE guidelines 2.0 and the "Guidelines for the Care and Use of Laboratory Animals", and approved by the Animal Ethics Committee of Wenzhou University (Issue No.WZU-2022-005). Female C57BL/6J mice (6-8 weeks old, 20-25 g) were purchased from the Wenzhou University Laboratory Animal Center (Wenzhou, Zhejiang, China). Mice were maintained with SPF food and water for 1−2 week. The animal room temperature is 20−26 ^{o}C, warm humidity 40−70%, 12 hours of light and darkness alternate and normal feeding before animal experiments, and mice should be fasted for 12 h to avoid fluorescence interference from foodstuff.

To explore the viscosity abnormalities in diseased mice, mice were randomly divided into three groups: normal group, inflammation group, and NASH group. The inflammation group mice were given an intraperitoneal injection of LPS (100 μL, 1 mg/mL) for 12 h. The NASH group were fed with a high-fat diet (methionine-choline deficient diet) plus injecting dexamethasone sodium phosphate (DEX, 15 mg/kg) intraperitoneally every other day for 18 days. In addition, mice in the NASH group were intraperitoneal injected with CCl_4 (0.5 mg/kg in olive oil) every other day from day 11 to end of day 18. The control mice were administered with normal diet and injected with 0.9% saline.

To evaluate biodistribution of **Cy-Vis2**, the normal mice were intravenously injected with **Cy-Vis2** (50 μM, 100 μL) solution in HEPES buffer-glycerin mixture solution (1:1, v/v). After 1.5 hour, the mice were sacrificed by cervical dislocation. The heart, liver, spleen, lung, and kidney were harvested and washed thoroughly with saline. The organs were subjected for imaging by using an optical imaging system (Perkin Elmer IVIS Lumina XRMS Series III).

Control and inflammation mice were administrated with **Cy-Vis2** (50 μM, 100 μL) in saline-glycerol mixture solution (1:1, v/v) by intraperitoneal injection and imaged. For NASH mice imaging, **Cy-Vis2** (50 μM, 100 μL) in saline-glycerol mixture solution (1:1, v/v) was injected intravenously into control and NASH mice via the tail vein. After an additional 1.5 h, the fluorescence imaging was performed in a Perkin Elmer IVIS Lumina XRMS Series III with $\lambda_{ex}/\lambda_{em}$ = 620 nm/790 nm.

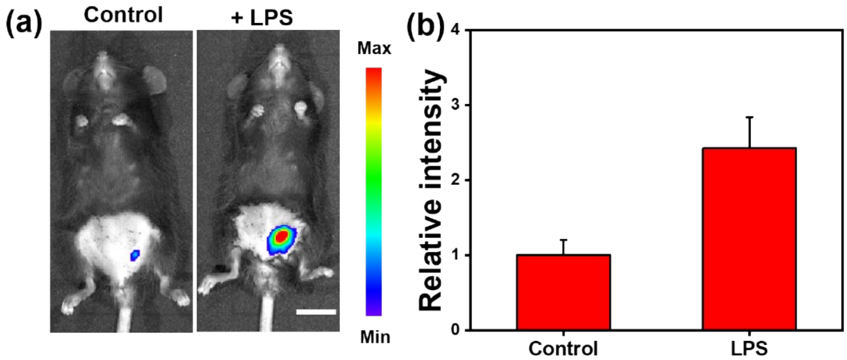

Fig. S20 In vivo fluorescence imaging of **Cy-Vis2** (100 μL, 50 μM) in mice. (a) Healthy and inflammation mice were imaged after injected with **Cy-Vis2**, scale bar is 1 cm, λ_{ex} = 620 nm, λ_{em} = 790 nm. (b) Relative fluorescence intensity obtained from (a), error bars represent the standard deviation (±SD, n = 3).

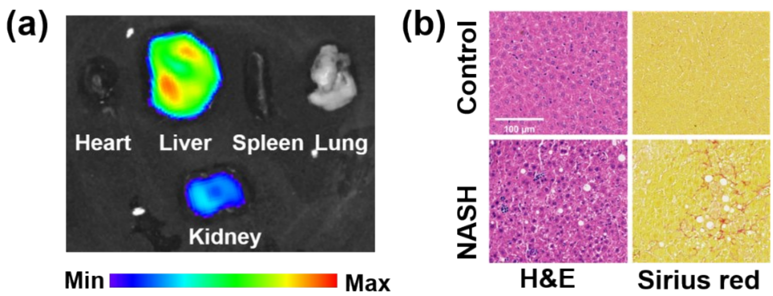

Fig. S21 (a) *Ex vivo* imaging of the organs isolated from the mice after intravenous injection of **Cy-Vis2**. (b) H&E and Sirius Red staining of liver tissues between normal and NASH mice, scale bar is 100 μm.

References

1. M. J. Frisch, G. W. Trucks, H. B. Schlegel, G. E. Scuseria, M. A. Robb, J. R. Cheeseman, G. Scalmani, V. Barone, G. A. Petersson, H. Nakatsuji, X. Li, M. Caricato, A. V. Marenich, J. Bloino, B. G. Janesko, R. Gomperts, B. Mennucci, H. P. Hratchian, J. V. Ortiz, A. F. Izmaylov, J. L. Sonnenberg, Williams, F. Ding, F. Lipparini, F. Egidi, J. Goings, B. Peng, A. Petrone, T. Henderson, D. Ranasinghe, V. G. Zakrzewski, J. Gao, N. Rega, G. Zheng, W. Liang, M. Hada, M. Ehara, K. Toyota, R. Fukuda, J. Hasegawa, M. Ishida, T. Nakajima, Y. Honda, O. Kitao, H. Nakai, T. Vreven, K. Throssell, J. A. Montgomery Jr., J. E. Peralta, F. Ogliaro, M. J. Bearpark, J. J. Heyd, E. N. Brothers, K. N. Kudin, V. N. Staroverov, T. A. Keith, R. Kobayashi, J.

Normand, K. Raghavachari, A. P. Rendell, J. C. Burant, S. S. Iyengar, J. Tomasi, M. Cossi, J. M. Millam, M. Klene, C. Adamo, R. Cammi, J. W. Ochterski, R. L. Martin, K. Morokuma, O. Farkas, J. B. Foresman, D. J. Fox, *Gaussian 16* (Gaussian, Inc., Wallingford CT, 2016).

2. W. Humphrey, A. Dalke, K. Schulten, VMD: visual molecular dynamics, *J. Mol. Graph*. 1996, **14**, 33-38.
3. S. Yao, Y. Chen, W. Ding, F. Xu, Z. Liu, Y. Li, Y. Wu, S. Li, W. He, Z. Guo, Single-atom engineering of hemicyanine and its amphiphilic derivative for optimized near infrared phototheranostics, *Chem. Sci.* 2023, **14**, 1234-1243.
4. M. Dashtiev, V. Azov, V. Frankevich, L. Scharfenberg, R. Zenobi, Clear evidence of fluorescence resonance energy transfer in gas-phase ions, *J. Am. Soc. Mass Spectrom*. 2005, **16**, 1481–1487.